Computation of TM and TE Modes in Waveguides Based on a Surface Integral Formulation

Madhavan Swaminathan, *Member, IEEE,* Tapan K. Sarkar, *Fellow, IEEE,* and Arlon T. Adams, *Senior Member, IEEE*

Abstract—**The surface integral formulation has been used here for the computation of TM and TE modes propagating in dielectric loaded waveguides. This formulation makes use of the surface equivalence principle whereby the field at any point internal or external to the waveguide can be expressed in terms of equivalent surface currents. This procedure reduces the original problem into a set of integro-differential equations which is then reduced to a matrix equation using method of moments. The solution of this matrix equation provides the propagation characteristics of the waveguide and the equivalent surface currents existing on the waveguide walls. The equivalent surface currents can be used to compute the fields at all points, both inside and outside the waveguide. The surface integral method has been used to compute the propagation characteristics of waves propagating in dielectric loaded waveguides. The computed results agree very well with analytical and published data. However, the use of the surface integral method on dielectric loaded waveguides sometimes leads to the existence of spurious modes. A method has been illustrated which can be used to remove these spurious modes.**

I. An Overview

A METHOD based on a surface integral formulation has been used here for the computation of TM_z and TE_z modes propagating in dielectric loaded waveguides. This formulation is based on the surface equivalence principle whereby the structure is modeled by equivalent surface currents that now represent the sources producing fields in an homogeneous medium. A method of moments technique has been used to compute the dispersion relation and the equivalent surface currents using which the fields at all points in and around the waveguide can be computed. The waveguide can now be easily modeled since the waveguide parameters can be calculated from the fields. The authors believe that the surface integral formulation used here is a very easy and effective technique to analyze waveguides having very complex geometries.

The surface integral method has been used in the past by Swaminathan *et al.* [1] and Spielman *et al.* [2] to analyze hollow waveguides. The method presented in this paper is an extension of [1].

Manuscript received October 1, 1990; revised March 11, 1991.

M. Swaminathan is with International Business Machines Corporation, East Fishkill, NY 12533.

T. K. Sarkar and A. T. Adams are with the Department of Electrical Engineering, Syracuse University, Syracuse, NY 13244-1240.

IEEE Log Number 9105250.

A dielectric loaded waveguide is made up of multiple conductors and dielectrics. Due to the presence of multiple dielectric mediums, no simple relation exists between the propagation constant and frequency. Hence, unlike a hollow waveguide [1], [2], the cutoff wavenumber alone cannot be used to completely characterise the dielectric loaded waveguide. Three types of modes can propagate in a waveguide namely, TM, TE and hybrid. This paper gives a detailed account of the use of the surface integral method to compute the TM and TE modes propagating in dielectric loaded waveguides.

II. Introduction

Consider a dielectric loaded waveguide of arbitrary cross section existing in free space, as shown in Fig. 1. The conductor and dielectric are non-touching and the space between them is filled with free space. The conductor is assumed to be a perfect electric conductor ($\sigma \to \infty$), thus making the tangential component of the electric field vanish on its surface. The waveguide is infinite along the z-direction and has a finite cross-section along the x-y plane. Since the waveguide is made up of multiple dielectric mediums, the permeability and permittivity of each dielectric differs from its surrounding medium.

Consider waves travelling along the z-direction in the dielectric loaded waveguide shown in Fig. 1. These waves can be represented by wavefunctions of the form

$$\psi_m = h_m(k_{xm})h_m(k_{ym})\, e^{-j\beta z} \qquad m = 0, 1 \qquad (1)$$

where ψ_m are wavefunctions in the mth medium, $h_m(k_{xm})$ and $h_m(k_{ym})$ are harmonic functions along the x and y directions respectively and k_{xm}, k_{ym} are separation parameters given by the separation equation $k_{xm}^2 + k_{ym}^2 + \beta^2 = k_m^2$. In (1), β is the propagation constant and k_m is the wavenumber in the mth dielectric medium given by $k_m = \omega\sqrt{\mu_m \epsilon_m}$, where ω is the angular frequency of the wave propagating in the waveguide and μ_m, ϵ_m are the permeability and permittivity of the mth medium respectively.

The wavefunctions ψ_m in (1) completely characterize the waveguide since these wavefunctions can be used to find the electric and magnetic fields at all points inside and outside the waveguide. Due to the presence of multiple dielectric regions, there is no simple relation between the propagation constant β and the cut-off wavenumber as was possible with the hollow waveguides [1], [2].

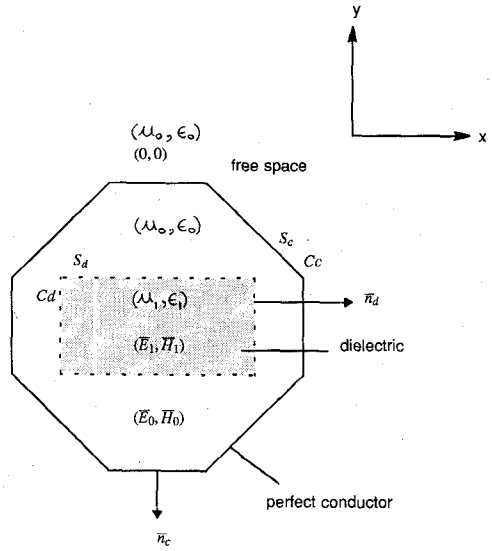

Fig. 1. Dielectric loaded waveguide.

Hence to get a relation between β and the wavenumber in free space k_0, it is necessary to satisfy the continuity of the tangential components of the electric and magnetic fields at any interface.

A surface integral formulation has been used here to characterise dielectric loaded waveguides. This formulation makes use of the surface equivalence principle to represent the waveguide by equivalent currents that produce the same fields as in the original problem. The problem is then reduced to an eigenvalue matrix equation and solved as in [1].

TM_z and TE_z modes can propagate in a dielectric loaded waveguide. TM_z and TE_z modes are characterized by the absence of the axial components of the magnetic field and electric field respectively.

III. Maxwell's Equations

The surface integral formulation uses equivalent sources to compute the electric and magnetic fields at all points both inside and outside the waveguide. This is achieved by applying the surface equivalence principle to the structure being analysed. The first step in the use of the surface equivalence principle to represent fields in terms of equivalent sources is to find the relation between the electric and magnetic fields at any point in the waveguide shown in Fig. 1.

For the waveguide shown in Fig. 1, Maxwell's equations hold for each medium and for the dielectric medium with material properties (μ_m, ϵ_m), is given by

$$\bar{\nabla} \times \bar{H}_m = j\omega\epsilon_m \bar{E}_m$$
$$\bar{\nabla} \times \bar{E}_m = -j\omega\mu_m \bar{H}_m \tag{2}$$

where $\bar{H}_m$, $\bar{E}_m$ are the magnetic field and electric field respectively in the mth medium. Equation (2) gives the relation between $\bar{E}_m$ and $\bar{H}_m$ at any point in the mth medium. Due to wave propagation along the z-direction, the fields vary as $e^{-j\beta z}$ along that direction, where β is the propagation constant of the wave.

Separating (2) into the longitudinal and transverse components and making some manipulations [3], the electric field can be rewritten in the form

$$\bar{E}_{zm} = \frac{1}{j\omega\epsilon_m} \bar{\nabla}_l \times \bar{H}_{lm}$$
$$\bar{E}_{lm} = -\frac{j\beta}{(k_m^2 - \beta^2)} \bar{z} \times \bar{\nabla}_l \times \bar{E}_{zm}$$
$$-\frac{j\omega\mu_m}{(k_m^2 - \beta^2)} \bar{\nabla}_l \times \bar{H}_{zm}. \tag{3}$$

In (3), $\bar{E}_{zm}$, $\bar{E}_{lm}$ are the longitudinal and transverse electric fields in the mth medium respectively, $\bar{H}_{zm}$, $\bar{H}_{lm}$ are the longitudinal and transverse magnetic field in the mth medium respectively and $\bar{\nabla}_l$ is the transverse $\bar{\nabla}$ operator.

For a TM_z mode propagating in the waveguide, the axial magnetic field is zero ($\bar{H}_{zm} = 0$) and hence the electric fields from (3) are

$$\bar{E}_{zm} = \frac{1}{j\omega\epsilon_m} \bar{\nabla}_l \times \bar{H}_{lm}$$
$$\bar{E}_{lm} = -\frac{j\beta}{(k_m^2 - \beta^2)} \bar{z} \times \bar{\nabla}_l \times \bar{E}_{zm}. \tag{4}$$

For a TE_z mode propagating in the waveguide, the axial electric field is zero ($\bar{E}_{zm} = 0$) and hence the electric fields from (3) are

$$\bar{E}_{zm} = 0$$
$$\bar{E}_{lm} = -\frac{j\omega\mu_m}{(k_m^2 - \beta^2)} \bar{\nabla}_l \times \bar{H}_{zm}. \tag{5}$$

IV. Source Field Relation

A wave propagating along the z-direction in the waveguide shown in Fig. 1 produces fields $\bar{E}_m$ and $\bar{H}_m$ in the mth medium. Let the entire space be filled with the material properties of the mth medium and let sources existing in this medium produce fields $\bar{E}_m$, $\bar{H}_m$ inside the boundary making up the mth medium and zero fields everywhere else. This equivalent problem is shown in Fig. 2 for the medium $m = 1$ and the equations derived in this section are necessary for applying the surface equivalence principle to the waveguide of Fig. 1.

Consider sources $\bar{J}$, $\bar{M}$ producing fields $\bar{E}_m$, $\bar{H}_m$ and (0, 0) in the homogeneous medium shown in Fig. 2. Here $\bar{J}$ and $\bar{M}$ represent the electric and magnetic sources respectively. The electric fields produced by these current sources can be evaluated by the method of superposition [3], [4]. Representing the electric and magnetic fields $\bar{E}_m$, $\bar{H}_m$ in (3), (4), (5) in terms of equivalent electric and magnetic sources $\bar{J}$, $\bar{M}$ [3] the following equations are obtained.

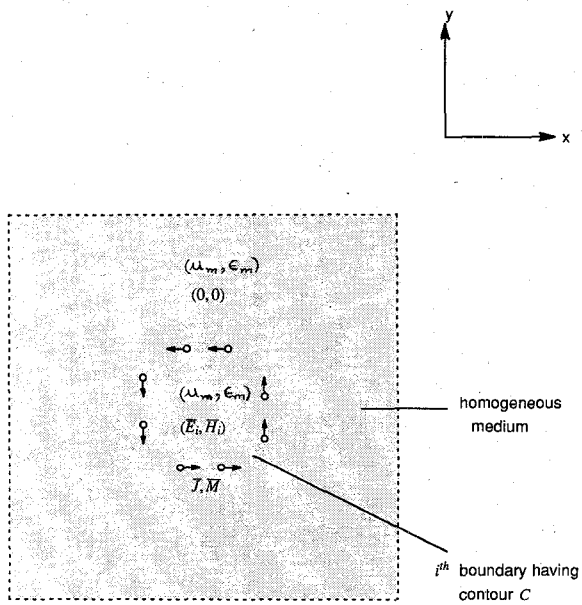

Fig. 2. Sources in a homogeneous infinite medium.

A. TM_z *Modes*

$$\bar{E}_{zm} = \frac{(k_m^2 - \beta^2)}{j\omega\epsilon_m}\bar{A}_{zm} - \bar{\nabla}_l \times \bar{F}_{lm}$$

$$\bar{E}_{lm} = -\frac{\beta}{\omega\epsilon_m}\bar{\nabla}_l A_{zm} - \bar{\nabla}_l \times \bar{F}_{zm} + j\beta\bar{z} \times \bar{F}_{lm}. \quad (6)$$

B. TE_z *Modes*

$$\bar{E}_{zm} = 0$$

$$\bar{E}_{lm} = -\frac{j\omega\mu_m}{(k_m^2 - \beta^2)}[(k_m^2 - \beta^2)\bar{A}_{lm} + \bar{\nabla}_l\phi_{lm}] - \bar{\nabla}_l \times \bar{F}_{zm}. \quad (7)$$

In equations (6), (7), $\bar{A}_{zm}$, $\bar{A}_{lm}$, ϕ_{lm}, $\bar{F}_{zm}$, $\bar{F}_{lm}$ represent the longitudinal magnetic vector potential, transverse magnetic vector potential, transverse electric scalar potential, longitudinal electric vector potential and transverse electric vector potential in the mth medium, respectively. These are given by

$$\bar{A}_{zm}; \bar{A}_{lm} = \frac{1}{4j}\oint_C \bar{J}H_0^{(2)}(\sqrt{k_m^2 - \beta^2}R)\, dl'$$

$$\phi_{lm} = \frac{1}{4j}\oint_C \bar{\nabla}_l' \cdot \bar{J}H_0^{(2)}(\sqrt{k_m^2 - \beta^2}R)\, dl'$$

$$\bar{F}_{zm}; \bar{F}_{lm} = \frac{1}{4j}\oint_C \bar{M}H_0^{(2)}(\sqrt{k_m^2 - \beta^2}R)\, dl'$$

where the electric current $\bar{J}$ is longitudinally directed for $\bar{A}_{zm}$ and transversely directed for $\bar{A}_{lm}$, ϕ_{lm} and the magnetic current $\bar{M}$ is longitudinally directed for $\bar{F}_{zm}$ and transversely directed for $\bar{F}_{lm}$. In the above equations, C represents the contour supporting the currents, $H_0^{(2)}$ is the zeroth order Hankel function of the second kind, R is the distance between the source and field points, the primed variables represent the source and the unprimed variables represent the field.

V. Integral Formulation

Consider the waveguide shown in Fig. 1 which is made up of one conductor and one dielectric, existing in free space. The material properties of free space and dielectric medium are (μ_0, ϵ_0) and (μ_1, ϵ_1), respectively. In Fig. 1, S_c represents the surface of the conductor, S_d is the surface of the dielectric and $\bar{n}_c$, $\bar{n}_d$ are the unit outward normals to surfaces S_c and S_d, respectively.

Let a wave propagate along the z-direction in the waveguide. This wave produces fields $(\bar{E}_0, \bar{H}_0)$ and $(\bar{E}_1, \bar{H}_1)$ in the space between S_c, S_d and inside S_d, respectively. Here $\bar{E}$ represents the electric field and $\bar{H}$ represents the magnetic field. Since the conductor is perfect and completely surrounds the dielectric, zero fields are produced by the wave at all points outside the surface S_c. This is represented by (0, 0) in Fig. 1.

The surface equivalence principle can now be used to represent the fields at all points in the waveguide by means of equivalent surface currents.

A. *Equivalence in Medium* (μ_0, ϵ_0)

The waveguide in Fig. 1 has been redrawn in Fig. 3. In this figure, the fields in the medium (μ_0, ϵ_0) remain as in Fig. 1 and the fields in medium (μ_1, ϵ_1) have been replaced by null fields. Due to the absence of any field inside the surface S_d, the entire space can now be filled with material properties of free space, namely (μ_0, ϵ_0).

Since the entire space is filled with the (μ_0, ϵ_0) medium and due to the jump in the tangential electric and magnetic fields on surfaces S_c and S_d, the waveguide can be represented by equivalent electric and magnetic currents which produce the fields (0, 0) outside S_c, $(\bar{E}_0, \bar{H}_0)$ in the space between S_c, S_d and (0, 0) inside S_d. These equivalent surface currents exist on surfaces S_c and S_d.

The magnitude of these surface currents are given by the discontinuity in the tangential electric and magnetic fields on surfaces S_c and S_d:

$$\bar{J}_c = -\bar{n}_c \times \bar{H}_0(S_c^-)$$

$$\bar{J}_d = \bar{n}_d \times \bar{H}_0(S_d^+)$$

$$\bar{M}_d = \bar{E}_0(S_d^+) \times \bar{n}_d. \quad (8)$$

In the above equations, $\bar{J}_c$ and $\bar{J}_d$ are the electric surface currents on surfaces S_c and S_d respectively, $\bar{M}_d$ is the magnetic surface current on surface S_d, $\bar{H}_0(S_c^-)$ is the magnetic field just inside surface S_c, $\bar{H}_0(S_d^+)$ is the magnetic field just outside surface S_d and $\bar{E}_0(S_d^+)$ is the electric field just outside surface S_d. No magnetic current exists on the surface of the conductor $(\sigma \to \infty)$ since the tangential electric field is zero on the surface of a perfect conductor.

The currents $\bar{J}_c$, $\bar{J}_d$ and $\bar{M}_d$ now act as sources producing the fields $(\bar{E}_0, \bar{H}_0)$ and (0, 0), at all points shown in Fig. 3.

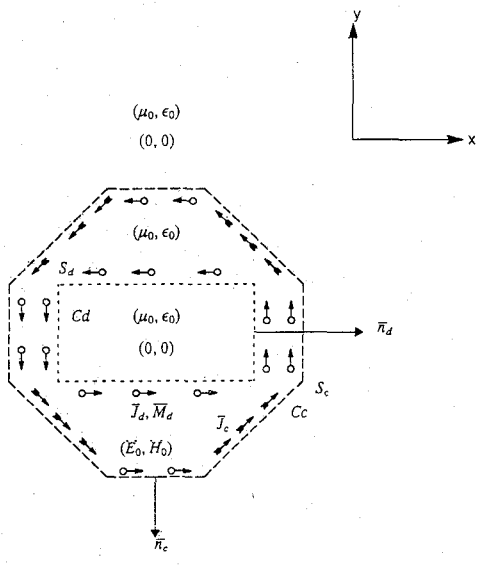

Fig. 3. Equivalence in medium.

From Fig. 3, the tangential electric and magnetic fields have to vanish on surfaces S_c^+ and S_d^-, which are the boundary conditions. Making use of only the electric fields, the boundary conditions are

$$\bar{n}_c \times \bar{E}_0 = 0 \quad \text{on } S_c^+$$
$$\bar{n}_d \times \bar{E}_0 = 0 \quad \text{on } S_d^-. \tag{9}$$

In (9), the electric fields are produced by the current sources $\bar{J}_c$, $\bar{J}_d$ and $\bar{M}_d$.

B. Equivalence in Medium (μ_1, ϵ_1)

The waveguide in Fig. 1 has been redrawn in Fig. 4 where the fields in region between S_c, S_d have been replaced by zero fields (0, 0) and the fields in the region inside S_d remain as $(\bar{E}_1, \bar{H}_1)$. Since the outer surface of the waveguide is made up of a perfect conductor, zero fields exist in the region outside the surface S_c. Since zero fields exist in the region between S_c, S_d and outside S_c, the entire space can be filled with the medium with material properties (μ_1, ϵ_1). This is shown in Fig. 4.

Due to the discontinuity in the tangential electric and magnetic fields on surface S_d, electric and magnetic currents exist on this surface whose magnitudes are given by

$$\bar{J}_d' = -\bar{n}_d \times \bar{H}_1(S_d^-)$$
$$\bar{M}_d' = -\bar{E}_1(S_d^-) \times \bar{n}_d. \tag{10}$$

As before, $\bar{E}_1(S_d^-)$ and $\bar{H}_1(S_d^-)$ are the electric and magnetic fields just inside the dielectric surface S_d.

The currents $\bar{J}_d'$, $\bar{M}_d'$ are the equivalent electric and magnetic current sources that produce the fields $(\bar{E}_1, \bar{H}_1)$ inside the surface S_d and zero fields at all other points, as shown in Fig. 4.

The tangential electric and magnetic fields have to vanish on the surface just outside S_d, which is the boundary condition. Using only the electric field, the boundary condition is

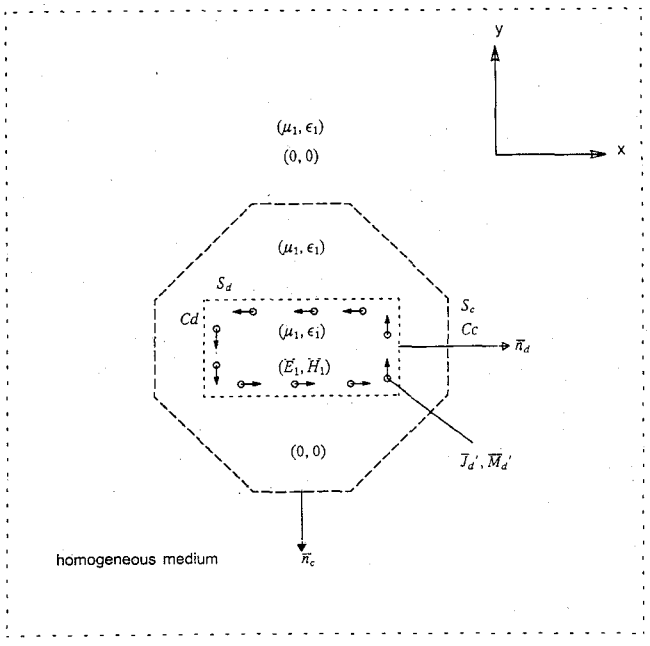

Fig. 4. Equivalence in medium.

$$\bar{n}_d \times \bar{E}_1 = 0 \quad \text{on } S_d^+. \tag{11}$$

In (11), $\bar{E}_1$ is the electric field produced by the surface currents $\bar{J}_d'$ and $\bar{M}_d'$.

C. Electric Field Equations

Equations (9) and (11) represent three equations in five unknowns. From the original waveguide problem in Fig. 1, due to the absence of currents on the waveguide walls, the tangential electric and magnetic fields have to be continuous on the surface S_d. Hence

$$\bar{n}_d \times \bar{E}_0 = \bar{n}_d \times \bar{E}_1$$
$$\bar{n}_d \times \bar{H}_0 = \bar{n}_d \times \bar{H}_1. \tag{12}$$

Making use of (8) and (10) in (12):

$$\bar{M}_d = -\bar{M}_d' \tag{13}$$
$$\bar{J}_d = -\bar{J}_d' \tag{14}$$

Hence (9) and (11) can be reduced to three equations in three unknowns which are

$$\left.\begin{aligned} \bar{n}_c \times \bar{E}_0(\bar{J}_c, \bar{J}_d, \bar{M}_d) &= 0 \quad \text{on } S_c^+ \\ \bar{n}_d \times \bar{E}_0(\bar{J}_c, \bar{J}_d, \bar{M}_d) &= 0 \quad \text{on } S_d^- \end{aligned}\right\} \text{ in medium } (\mu_0, \epsilon_0)$$
$$\bar{n}_d \times \bar{E}_1(-\bar{J}_d, -\bar{M}_d) = 0 \quad \text{on } S_d^+ \quad \text{in medium } (\mu_1, \epsilon_1). \tag{15}$$

Equation (15) is the electric field integral equation that can be used to characterize the waveguide in Fig. 1 which is made up of one conductor and one dielectric. In (15), the electric fields produced by the various sources are given by either (4) or (5) depending on whether a TM_z or TE_z mode is propagating in the waveguide.

For a waveguide containing N_c conductors and N_d dielectrics ([3]), the number of equations and unknowns in the electric field integral equation is $N_c + 2N_d$.

VI. Method of Moments

Method of moments [5] can be used to reduce (15) to a matrix equation, which can then be numerically solved on a computer.

Based on [5] and Figs. 5 and 6, the currents are expanded as

$$\bar{J}_c = \sum_{i=1}^{n} I_i \bar{J}_i$$

$$\bar{J}_d = \sum_{i=n+1}^{n+m} I_i \bar{J}_i$$

$$\bar{M}_d = \sum_{i=n+m+1}^{n+2m} I_i \bar{M}_{i-m} \tag{16}$$

and the weighting functions as

$$\bar{W}_c = \sum_{k=1}^{n} \bar{W}_k; \qquad \bar{W}_d = \sum_{k=n+1}^{n+m} \bar{W}_k. \tag{17}$$

Expanding the currents $\bar{J}_c$, $\bar{J}_d$, $\bar{M}_d$ in terms of expansion functions (16) and testing equation (15) with the set of weighting functions (17), [3], [5], a matrix equation of the form

$$[Z][I] = [0] \tag{18}$$

is obtained where $[Z]$ is a square matrix and $[I]$ is a vector with elements representing the current coefficients.

In this paper, pulses have been used as the expansion functions for the currents and a set of delta functions have been used as the weighting functions.

VII. TM Formulation

Let a TM_z mode propagate in the waveguide shown in Fig. 1. Since no explicit relation exists between the propagation constant β and the wavenumber in free space, a set of equations have to be solved to get this relation.

Equation (6) for $\bar{E}_{zm}$ can be used to compute the relation between β and the wavenumber in free space k_0.

$$\bar{J}_i = P_i(l' - l_{i-1})\bar{z}_i' \qquad i = 1, 2, \cdots, n \tag{19}$$

$$P_i(l' - l_{i-1}) = \begin{cases} 1 & 0 \le l' - l_{i-1} \le l_i - l_{i-1} \\ 0 & \text{otherwise} \end{cases}$$

$$\bar{J}_i = P_i(l' - l_i)\bar{z}_i'$$

$$i = n + 1, n + 2, \cdots, n + m \tag{20}$$

$$P_i(l' - l_i) = \begin{cases} 1 & 0 \le l' - l_i \le l_{i+1} - l_i \\ 0 & \text{otherwise} \end{cases}$$

$$\bar{M}_{i-m} = P_{i-m}(l' - l_{i-m})\bar{l}'_{i-m}$$

$$i = n + m + 1, \cdots, n + 2m$$

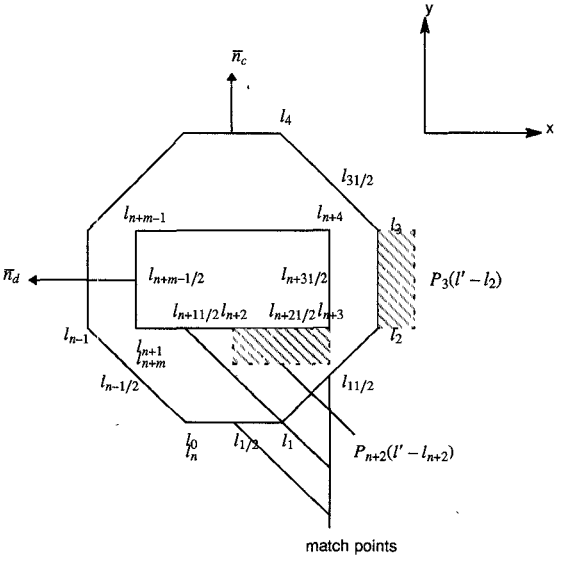

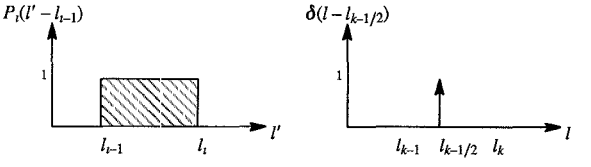

Fig. 5. Patching details for TM formulation.

$$P_{i-m}(l' - l_{i-m}) = \begin{cases} 1 & 0 \le l' - l_{i-m} \le l_{i-m+1} \\ & \quad - l_{i-m} \\ 0 & \text{otherwise} \end{cases} \tag{21}$$

In the above equations, $\bar{z}_i'$ and $\bar{l}'_{i-m}$ are unit tangential vectors on the ith and $(i - m)$th subsection supporting the electric and magnetic currents respectively. The former is the axially directed unit vector and the latter is the transversely directed unit vector.

The weighting functions are chosen to be delta functions which can be represented as

$$\bar{W}_k = \delta(l - l_{k-1/2})\,\Delta l_k \bar{z}_k$$

$$k = 1, 2, \cdots, n \tag{22}$$

$$\delta(l - l_{k-1/2}) = \begin{cases} 1 & l = l_{k-1/2} \\ 0 & \text{otherwise} \end{cases}$$

$$\Delta l_k = l_k - l_{k-1}; \qquad l_{k-1/2} = \frac{l_k + l_{k-1}}{2} \tag{23}$$

$$\bar{W}_k = \delta(l - l_{k+1/2})\,\Delta l_k \bar{z}_k$$

$$k = n + 1, \quad n + 2, \cdots, n + m \tag{24}$$

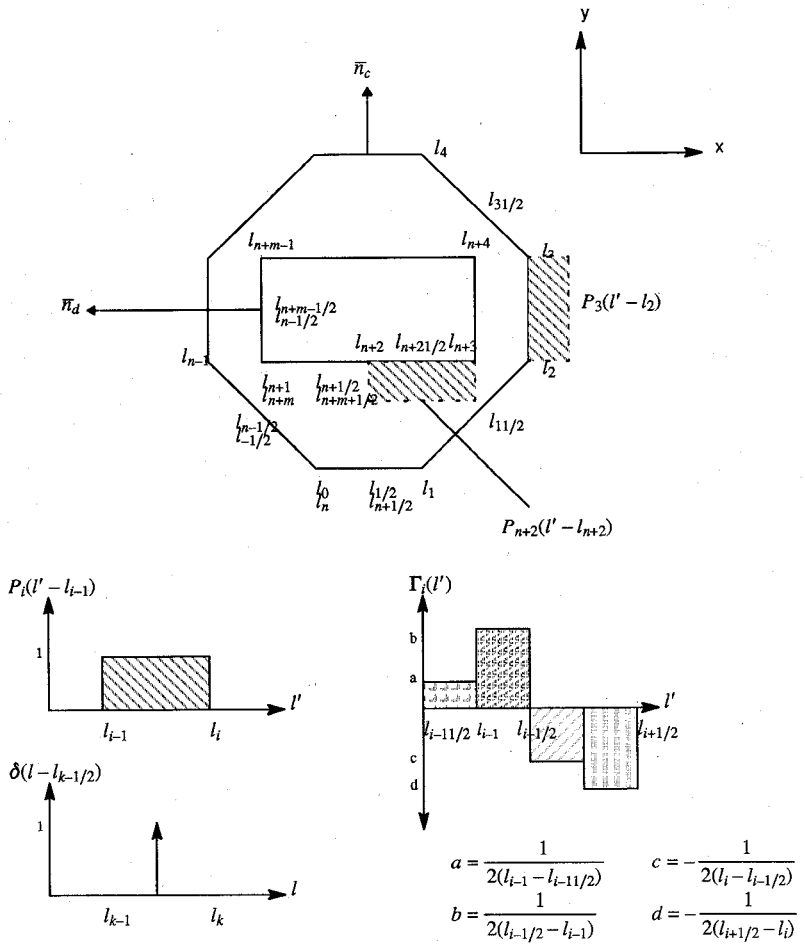

Fig. 6. Patching details for TE formulation.

$$\delta(l - l_{k+1/2}) = \begin{cases} 1 & l = l_{k+1/2} \\ 0 & \text{otherwise} \end{cases}$$

$$\Delta l_k = l_{k+1} - l_k; \qquad l_{k+1/2} = \frac{l_{k+1} + l_k}{2}. \quad (25)$$

As before, $\bar{z}_k$ is the axially directed unit vector on the kth subsection supporting the kth weighting function.

Expanding the currents in (6) and testing (6) with the weighting functions ([3]) reduces it to the form

$$-\Delta l_k \frac{(k_0^2 - \beta^2)}{4\omega\epsilon_0} \sum_{i=1}^{n} I_i \int_{l_{i-1}}^{l_i} \delta(l - l_{k-1/2}) P_i(l' - l_{i-1}) \cdot H_0^{(2)}(\sqrt{k_0^2 - \beta^2} R)\, dl' - \Delta l_k \frac{(k_0^2 - \beta^2)}{4\omega\epsilon_0} \sum_{i=n+1}^{n+m} I_i \cdot \int_{l_i}^{l_{i+1}} \delta(l - l_{k-1/2}) P_i(l' - l_i) H_0^{(2)}(\sqrt{k_0^2 - \beta^2} R)\, dl' + \Delta l_k \frac{\sqrt{k_0^2 - \beta^2}}{4j} \sum_{i=n+m+1}^{n+2m} I_i \int_{l_{i-m}}^{l_{i-m+1}} \left(\frac{\overline{R}}{R} \cdot \bar{n}'_{i-m}\right) \cdot \delta(l - l_{k-1/2}) P_{i-m}(l' - l_{i-m}) \cdot H_1^{(2)}(\sqrt{k_0^2 - \beta^2} R)\, dl' = 0 \qquad k = 1, 2, \cdots, n$$

$$-\Delta l_k \frac{(k_0^2 - \beta^2)}{4\omega\epsilon_0} \sum_{i=1}^{n} I_i \int_{l_{i-1}}^{l_i} \delta(l - l_{k+1/2}) \cdot P_i(l' - l_{i-1}) H_0^{(2)}(\sqrt{k_0^2 - \beta^2} R)\, dl' - \Delta l_k \frac{(k_0^2 - \beta^2)}{4\omega\epsilon_0} \cdot \sum_{i=n+1}^{n+m} I_i \int_{l_i}^{l_{i+1}} \delta(l - l_{k+1/2}) P_i(l' - l_i) \cdot H_0^{(2)}(\sqrt{k_0^2 - \beta^2} R)\, dl' + \Delta l_k \frac{\sqrt{k_0^2 - \beta^2}}{4j} \sum_{i=n+m+1}^{n+2m} I_i \cdot \int_{l_{i-m}}^{l_{i-m+1}} \left(\frac{\overline{R}}{R} \cdot \bar{n}'_{i-m}\right) \delta(l - l_{k+1/2}) P_{i-m}(l' - l_{i-m}) \cdot H_0^{(2)}(\sqrt{k_0^2 - \beta^2} R)\, dl' = 0$$

$$k = n + 1, \cdots, n + m$$

$$\Delta l_k \frac{(k_1^2 - \beta^2)}{4\omega\epsilon_1} \sum_{i=m+1}^{n+m} I_i \int_{l_i}^{l_{i+1}} \delta(l - l_{k+1/2}) P_i(l' - l_i) \cdot H_0^{(2)}(\sqrt{k_1^2 - \beta^2} R)\, dl' - \Delta l_k \frac{\sqrt{k_1^2 - \beta^2}}{4j} \sum_{i=n+m+1}^{n+2m} I_i \cdot \int_{l_{i-m}}^{l_{i-m+1}} \left(\frac{\overline{R}}{R} \cdot \bar{n}'_{i-m}\right) \delta(l - l_{k+1/2}) P_{i-m}(l' - l_{i-m}) \cdot H_1^{(2)}(\sqrt{k_1^2 - \beta^2} R)\, dl' = 0$$

$$k = n + 1, \cdots, n + m. \quad (26)$$

At a certain frequency ω and a fixed value of the propagation constant β (26) is a matrix equation of the form (18) where $[Z]$ is a $(n + 2m) \times (n + 2m)$ matrix and $[I]$ is a $(n + 2m) \times 1$ vector with elements $I_1, I_2, \cdots, I_n, \cdots, I_{n+m}, \cdots, I_{n+2m}$. In (26), $\bar{n}'_{i-m}$ is the unit outward normal to the $(i - m)$th segment supporting the magnetic current $\bar{M}_{i-m}$, $H_1^{(2)}$ is the first order Hankel function of the second kind, $\bar{R}$ is the vector from the source to the field point and R is the distance between the source and field points. In (26), all primed variables represent the source and all unprimed variables represent the field.

VIII. TE Formulation

Let a TE_z mode propagate in the waveguide shown in Fig. 1. This mode is characterised by the absence of the electric field along the axial direction of the waveguide. The transverse electric field produced by equivalent surface currents on the waveguide contour is given by (7).

The relation between the propagation constant β and the free space wavenumber k_0 can be obtained by solving the electric field integral equation obtained by substituting (7) into (15).

In the above equations, the electric currents $\bar{J}_c$, $\bar{J}_d$ are transversely directed and the magnetic current $\bar{M}_d$ is axially directed.

The expansion functions have been chosen to be pulses:

$$\bar{J}_i = P_i(l' - l_{i-1})\bar{l}'_i \qquad i = 1, 2, \cdots, n \tag{27}$$

$$P_i(l' - l_{i-1}) = \begin{cases} 1 & 0 \le l' - l_{i-1} \le l_i - l_{i-1} \\ 0 & \text{otherwise} \end{cases}$$

$$\bar{J}_i = P_i(l' - l_i)\bar{l}'_i \tag{28}$$

$$i = n + 1, \quad n + 2, \cdots, n + m$$

$$P_i(l' - l_i) = \begin{cases} 1 & 0 \le l' - l_i \le l_{i+1} - l_i \\ 0 & \text{otherwise} \end{cases}$$

$$\bar{M}_{i-m} = P_{i-m}(l' - l_{i-m})\bar{z}'_{i-m}$$

$$i = n + m + 1, \cdots, n + 2m \tag{29}$$

$$P_{i-m}(l' - l_{i-m}) = \begin{cases} 1 & 0 \le l' - l_{i-m} \le l_{i-m+1} \\ & \quad - l_{i-m} \\ 0 & \text{otherwise} \end{cases}$$

In the above equations, $\bar{l}'_i$ and $\bar{z}'_{i-m}$ are unit tangential vectors on the ith and $(i - m)$th subsection supporting the electric and magnetic currents respectively. The former is the transversely directed unit vector and the latter is the axially directed unit vector.

Using the expansion functions defined above, the divergence of the electric current which represents the charge is expanded as

$$\bar{\nabla}'_l \cdot \bar{J}_c = \sum_{i=1}^{n} I_i \Gamma_i(l') \tag{30}$$

$$\bar{\nabla}'_l \cdot \bar{J}_d = \sum_{i=n+1}^{n+m} I_i \Gamma_i(l') \tag{31}$$

where

$$\Gamma_i(l') = \begin{cases} \dfrac{1}{2(l_{i-1} - l_{i-1/2})} & l_{i-1/2} \le l' \le l_{i-1} \\ \dfrac{1}{2(l_{i-1/2} - l_{i-1})} & l_{i-1} \le l' \le l_{i-1/2} \\ \dfrac{-1}{2(l_i - l_{i-1/2})} & l_{i-1/2} \le l' \le l_i \\ \dfrac{-1}{2(l_{i+1/2} - l_i)} & l_i \le l' \le l_{i+1/2} \\ i = 1, 2, \cdots, n \end{cases} \tag{32}$$

$$\Gamma_i(l') = \begin{cases} \dfrac{1}{2(l_i - l_{i-1/2})} & l_{i-1/2} \le l' \le l_i \\ \dfrac{1}{2(l_{i+1/2} - l_i)} & l_i \le l' \le l_{i+1/2} \\ \dfrac{-1}{2(l_{i+1} - l_{i+1/2})} & l_{i+1/2} \le l' \le l_{i+1} \\ \dfrac{-1}{2(l_{i+1/2} - l_{i+1})} & l_{i+1} \le l' \le l_{i+1/2} \\ i = n + 1, \cdots, n + m \end{cases} \tag{33}$$

An approximation has been made while choosing the expansion functions for the divergence of the electric current in the above equations [3].

A set of delta functions have been used as the weighting functions.

$$\bar{W}_k = \delta(l - l_{k-1/2})\,\Delta l_k \bar{l}_k$$

$$k = 1, 2, \cdots, n \tag{34}$$

$$\delta(l - l_{k-1/2}) = \begin{cases} 1 & l = l_{k-1/2} \\ 0 & \text{otherwise} \end{cases}$$

$$\Delta l_k = l_k - l_{k-1}; \qquad l_{k-1/2} = \frac{l_k + l_{k-1}}{2} \tag{35}$$

$$\bar{W}_k = \delta(l - l_{k+1/2})\,\Delta l_k \bar{l}_k$$

$$k = n + 1, \quad n + 2, \cdots, n + m \tag{36}$$

$$\delta(l - l_{k+1/2}) = \begin{cases} 1 & l = l_{k+1/2} \\ 0 & \text{otherwise} \end{cases}$$

$$\Delta l_k = l_{k+1} - l_k; \qquad l_{k+1/2} = \frac{l_{k+1} + l_k}{2}. \tag{37}$$

As before, $\bar{l}_k$ is the transversely directed unit vector on the kth subsection supporting the kth weighting function.

Fig. 6 shows the representation of the expansion and weighting functions for a dielectric loaded waveguide supporting a TE_z mode.

Using the expansion functions, weighting functions and method of moments ([5]), (7) can be written in the form

$$-\frac{j\omega\mu_0}{(k_0^2-\beta^2)}\left[(k_0^2-\beta^2)\overline{W}_k^*\cdot\bar{A}_{l0}+\overline{W}_k^*\cdot\bar{\nabla}_l\phi_{l0}\right]-\overline{W}_k^*\cdot\bar{\nabla}_l\times\bar{F}_{z0}=0\qquad k=1,2,\cdots,n$$

$$-\frac{j\omega\mu_0}{(k_0^2-\beta^2)}\left[(k_0^2-\beta^2)\overline{W}_k^*\cdot\bar{A}_{l0}+\overline{W}_k^*\cdot\bar{\nabla}_l\phi_{l0}\right]-\overline{W}_k^*\cdot\bar{\nabla}_l\times\bar{F}_{z0}=0$$

$$k=n+1,n+2,\cdots,n+m$$

$$-\frac{j\omega\mu_1}{(k_1^2-\beta^2)}\left[(k_1^2-\beta^2)\overline{W}_k^*\cdot\bar{A}_{l1}+\overline{W}_k^*\cdot\bar{\nabla}_l\phi_{l1}\right]-\overline{W}_k^*\cdot\bar{\nabla}_l\times\bar{F}_{z1}=0$$

$$k=n+1,n+2,\cdots,n+m \tag{38}$$

where

$$\overline{W}_k^*\cdot\bar{A}_{l0}=\frac{\Delta l_k}{4j}\sum_{i=1}^{n}I_i\int_{l_{i-1}}^{l_i}\delta(l-l_{k-1/2})\cdot P_i(l'-l_{i-1})(\bar{l}_k\cdot\bar{l}_i')H_0^{(2)}(\sqrt{k_0^2-\beta^2}R)\,dl'+\frac{\Delta l_k}{4j}\sum_{i=n+1}^{n+m}I_i\int_{l_i}^{l_{i+1}}\delta(l-l_{k-1/2})\cdot P_i(l'-l_i)(\bar{l}_k\cdot\bar{l}_i')H_0^{(2)}(\sqrt{k_0^2-\beta^2}R)\,dl'$$

$$k=1,2,\cdots,n \tag{39}$$

$$\overline{W}_k^*\cdot\bar{A}_{l0}=\frac{\Delta l_k}{4j}\sum_{i=1}^{n}I_i\int_{l_{i-1}}^{l_i}\delta(l-l_{k+1/2})\cdot P_i(l'-l_{i-1})(\bar{l}_k\cdot\bar{l}_i')H_0^{(2)}(\sqrt{k_0^2-\beta^2}R)\,dl'+\frac{\Delta l_k}{4j}\sum_{i=n+1}^{n+m}I_i\int_{l_i}^{l_{i+1}}\delta(l-l_{k+1/2})\cdot P_i(l'-l_i)(\bar{l}_k\cdot\bar{l}_i')H_0^{(2)}(\sqrt{k_0^2-\beta^2}R)\,dl'$$

$$k=n+1,\cdots,n+m \tag{40}$$

$$\overline{W}_k^*\cdot\bar{A}_{l1}=-\frac{\Delta l_k}{4j}\sum_{i=n+1}^{n+m}I_i\int_{l_i}^{l_{i+1}}\delta(l-l_{k+1/2})\cdot P_i(l'-l_i)(\bar{l}_k\cdot\bar{l}_i')H_0^{(2)}(\sqrt{k_1^2-\beta^2}R)\,dl'$$

$$k=n+1,\cdots,n+m \tag{41}$$

$$\overline{W}_k^*\cdot\bar{\nabla}_l\phi_{l0}=\frac{1}{4j}\sum_{i=1}^{n}I_i\int_{l_i-11/2}^{l_i+1/2}(\delta(l-l_k)-\delta(l-l_{k-1}))\Gamma_i(l')H_0^{(2)}(\sqrt{k_0^2-\beta^2}R)\,dl'+\frac{1}{4j}\sum_{i=n+1}^{n+m}I_i\int_{l_i-1/2}^{l_i+11/2}(\delta(l-l_k)-\delta(l-l_{k-1}))\Gamma_i(l')H_0^{(2)}(\sqrt{k_0^2-\beta^2}R)\,dl'$$

$$k=1,2,\cdots,n \tag{42}$$

$$\overline{W}_k^*\cdot\bar{\nabla}_l\phi_{l0}=\frac{1}{4j}\sum_{i=1}^{n}I_i\int_{l_i-11/2}^{l_i+1/2}(\delta(l-l_{k+1})-\delta(l-l_k))\Gamma_i(l')H_0^{(2)}(\sqrt{k_0^2-\beta^2}R)\,dl'+\frac{1}{4j}\sum_{i=n+1}^{n+m}I_i\int_{l_i-1/2}^{l_i+11/2}(\delta(l-l_{k+1})-\delta(l-l_k))\Gamma_i(l')H_0^{(2)}(\sqrt{k_0^2-\beta^2}R)\,dl'$$

$$k=n+1,\cdots,n+m \tag{43}$$

$$\overline{W}_k^*\cdot\bar{\nabla}_l\phi_{l1}=-\frac{1}{4j}\sum_{i=n+1}^{n+m}I_i\int_{l_i-1/2}^{l_i+11/2}(\delta(l-l_{k+1})-\delta(l-l_k))\Gamma_i(l')H_0^{(2)}(\sqrt{k_1^2-\beta^2}R)\,dl'$$

$$k=n+1,\cdots,n+m \tag{44}$$

$$\overline{W}_k^*\cdot\bar{\nabla}_l\times\bar{F}_{z0}=\frac{\sqrt{k_0^2-\beta^2}}{4j}\Delta l_k\sum_{i=n+m+1}^{n+2m}\cdot I_i\int_{l_i-m}^{l_i-m+1}\left(\frac{\overline{R}}{R}\cdot\bar{n}_k\right)\delta(l-l_{k-1/2})\cdot P_{i-m}(l'-l_{i-m})\cdot H_1^{(2)}(\sqrt{k_0^2-\beta^2}R)\,dl'$$

$$k=1,2,\cdots,n \tag{45}$$

$$\overline{W}_k^*\cdot\bar{\nabla}_l\times\bar{F}_{z0}=\frac{\sqrt{k_0^2-\beta^2}}{4j}\Delta l_k\sum_{i=n+m+1}^{n+2m}\cdot I_i\int_{l_i-m}^{l_i-m+1}\left(\frac{\overline{R}}{R}\cdot\bar{n}_k\right)\delta(l-l_{k+1/2})\cdot P_{i-m}(l'-l_{i-m})\cdot H_1^{(2)}(\sqrt{k_0^2-\beta^2}R)\,dl'$$

$$k=n+1,\cdots,n+m \tag{46}$$

$$\overline{W}_k^*\cdot\bar{\nabla}_l\times\bar{F}_{z1}=-\frac{\sqrt{k_1^2-\beta^2}}{4j}\Delta l_k\sum_{i=n+m+1}^{n+2m}\cdot I_i\int_{l_i-m}^{l_i-m+1}\left(\frac{\overline{R}}{R}\cdot\bar{n}_k\right)\delta(l-l_{k+1/2})\cdot P_{i-m}(l'-l_{i-m})\cdot H_1^{(2)}(\sqrt{k_1^2-\beta^2}R)\,dl'$$

$$k=n+1,\cdots,n+m. \tag{47}$$

In (42), (43), (44), a finite difference operator has been used to represent the gradient operator $\overline{\nabla}_t$. The unit vector $\overline{n}_k$ is the unit outward normal on the kth subsection supporting the kth weighting function. As in the earlier sections, the primed variables represent the source, the unprimed variables represent the field and $H_1^{(2)}$ is the first order Hankel function of the second kind.

At a certain frequency ω and fixed propagation constant β, (38) becomes a matrix equation of the form (18).

IX. β-ω Relation

The propagation constant curve represents the variation of the propagation constant β with frequency ω or with the free space wavelength λ_0.

As explained earlier, at any fixed ω and β, the waveguide in Fig. 1 supporting a TM_z or TE_z mode can be reduced to the matrix equation

$$[Z][I] = [0]. \tag{48}$$

Assuming the above equation does represent a mode propagating in the waveguide, a non-trivial solution has to exist for the equivalent surface currents since the fields are not zero inside the waveguide. Since the vector $[I]$ represents the current coefficients, a non-trivial solution has to exist for the vector $[I]$ due to which the matrix $[Z]$ has to be singular. Hence

$$\det [Z] = 0. \tag{49}$$

Equation (49) is the same as the condition derived for a hollow conducting waveguide supporting a mode in [1]. Equations (48) and (49) can therefore be represented in the simpler form

$$[Z][I] = \lambda_{min}[I] \tag{50}$$

where λ_{min} is the minimum absolute eigenvalue of the matrix $[Z]$ and $[I]$ is the associated eigenvector. Based on (50), a mode exists for a certain ω and β if the minimum eigenvalue λ_{min} is zero which represents the singular condition (49).

A scanning procedure has been used here to obtain the β-ω curve. Consider the waveguide shown in Fig. 1. This guide is made up of a perfect conductor completely covering a dielectric with material properties (μ_1, ϵ_1). Since the perfect conductor completely covers the dielectric, β is a purely real quantity. Also if the wavenumber in free space is represented by k_0 and if the material is non-magnetic ($\mu_1 = \mu_0$) then β takes on values between

$$0 \le \beta \le k_0; \qquad k_0 \le \beta \le \sqrt{\epsilon_{r1}}k_0 \tag{51}$$

where $\epsilon_1 = \epsilon_0\epsilon_{r1}$. Based on this range, β can be fixed at some value and the wavenumber k_0 or wavelength λ_0 scanned over the range given in equation (51) to obtain the propagation curve. The wavelength λ_0 (for a fixed β) at which the absolute value of the minimum eigenvalue λ_{min} is minimum gives the relation between λ_0 and β.

Based on relation (51), it may be much easier to normalize β with respect to k_0 and fix this quantity. The range taken for this normalized β is

$$0 \le \overline{\beta} \le 1; \qquad 1 \le \overline{\beta} \le \sqrt{\epsilon_1} \tag{52}$$

where $\overline{\beta} = \beta/k_0$. The freespace wavelength λ_0 can now be scanned to find the value of λ_0 at which absolute λ_{min} is minimum. This technique however led to large errors in some cases. Hence it is worthwhile to note that fixing β instead of $\overline{\beta}$ produced much better results.

The matrix $[Z]$ used in the matrix equation is an unsymmetric, complex matrix. Hence the eigenvalues of this matrix are complex and so are the corresponding eigenvectors.

The eigenvector corresponding to any point on the propagation constant curve represents the equivalent currents existing on the surface of the waveguide. Since the currents represent the discontinuity in the tangential electric and magnetic fields, the eigenvector represents the tangential electric and magnetic fields on the surface of the waveguide. These tangential electric and magnetic fields on the waveguide surface represent the exact fields on the guide supporting the mode. The fields inside the waveguide can be found by following a reverse procedure whereby the vector $[I]$ can be used in the electric field integral equations to solve for the fields everywhere.

X. Results

A. Partially Filled Circular Guide

Fig. 7 shows a partially filled circular waveguide which is made up of an outer conductor and an inner dielectric shell, existing in free space. This guide can support a TM_z mode.

Since the conductor completely covers the dielectric shell, a wave propagating in this guide does not radiate any fields into the space outside the guide. An analytical solution exists for the relation between the propagation constant β and the free space wavenumber k_0 which is the solution to a characteristic equation [4].

A total of 50 subsections were used to model the waveguide shown in Fig. 7 of which 20 were used to model the conductor, 20 to model the outer surface of the dielectric shell and 10 to model the inner surface. This produced a total of 80 unknowns of which 20 represented the electric surface currents $\overline{J}_c$, 30 represented the dielectric surface currents $\overline{J}_d$ and 30 represented the magnetic surface currents $\overline{M}_d$. The surface integral formulation was used to obtain the $\beta - k_0$ relation for the waveguide supporting a TM_z mode. Fig. 8 shows this relation for the first TM_z mode for two relative dielectric constants $\epsilon_r = 2.54$ and $\epsilon_r = 10.2$. The star represents the exact solution which agrees well with the computed data.

The eigenvector at cut-off is shown in Fig. 9 which represents the tangential electric and magnetic fields on the surfaces of the conductor and dielectric shell. The x-axis represents the unknown and the y-axis is the corresponding current coefficient. Both the real and imaginary parts of the current coefficient have been plotted in Fig. 9. The

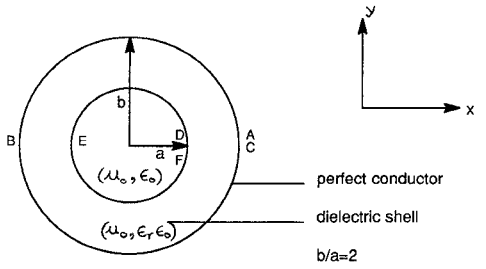

Fig. 7. Partially filled circular guide.

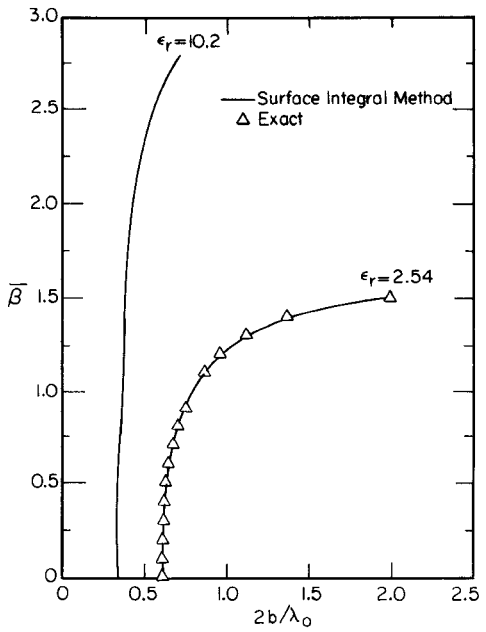

Fig. 8. Propagation constant curve of partially filled circular guide.

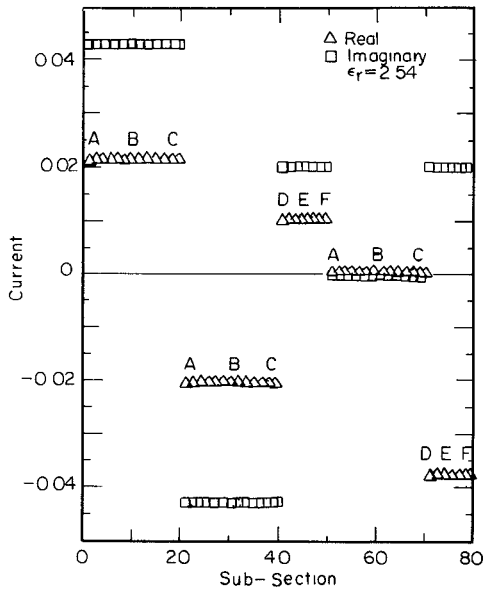

Fig. 9. Eigenvector distribution of partially filled circular guide.

manner in which the 80 unknowns have been split into conductor and dielectric currents are given below.

1–20 $\equiv \bar{J}_c$ on the surface of the conductor

21–40 $\equiv \bar{J}_d$ on the surface of the dielectric shell

41–50 $\equiv \bar{J}_d$ on the inner surface of the dielectric shell

51–70 $\equiv \bar{M}_d$ on the outer surface of the dielectric shell

71–80 $\equiv \bar{M}_d$ on the inner surface of the dielectric shell.

Based on the analytical solution, there can be no circumferential (ϕ) variation of the electric and magnetic fields for a TM_z mode propagating in the filled circular guide of Fig. 7. Since the equivalent surface currents represent the tangential electric and magnetic currents, they do not show any ϕ variation as can be seen from the constant eigenvector over any surface in Fig. 9. Moreover, since the tangential electric field is zero on the surface of the conductor, the magnetic currents representing numbers 51–70 are all zero (see Fig. 9). Since the outer surface of the dielectric shell touches the conductor, the currents $\bar{J}_c$, $\bar{J}_d$ should be equal and opposite as can be verified from Fig. 9.

B. Centered Dielectric Slab Waveguide

Fig. 10 shows a waveguide made up of an outer conductor and an inner centered dielectric slab. This waveguide supports a TE_z mode. An analytical solution exists for the β-ω relation which is given by the solution to a transcendental equation [4]. The dominant mode propagating in this waveguide is a TE_{10} mode.

The surface integral formulation was used to obtain the propagation constant curve for the guide shown in Fig. 10. A total of 102 unknowns were used to obtain the β-ω relation of which 58 represented the conductor electric surface current $\bar{J}_c$, 22 represented the dielectric electric surface current $\bar{J}_d$ and 22 represented the dielectric magnetic surface current $\bar{M}_d$. The β-ω relation obtained for the first two TE_z modes propagating in the waveguide have been plotted in Fig. 11. The star represents the values obtained from the analytical solution.

The distribution of the eigenvector at cutoff is shown in Fig. 12. As in the previous section, the x-axis represents the number of the unknown and the y-axis represents the corresponding current coefficient I. Both the real and imaginary part of the current coefficient have been shown in the figure. From the analytical solution, the electric and magnetic fields show no variation along the x-direction and show a sinusoidal variation along the y-direction. Since the surface currents represent the tangential electric and magnetic fields, they should show the same variation. From Fig. 12, there is no variation of the current $\bar{J}_c$ in regions $A - B$, $E - F$, $\bar{J}_c$ varies in a sinusoidal manner in regions $B - C - D - E$, $F - G - H - A$ and $\bar{J}_d$, $\bar{M}_d$ show no variation in regions $H - C$, $G - D$. The magnetic current $\bar{M}_d$ is zero in regions $C - D$, $G - H$ since the tangential electric field is zero on a perfect conductor. Hence the surface currents show the same distribution as the tangential fields obtained from an exact solution.

C. Insulated Finline

Fig. 13 shows an insulated finline. The dominant mode propagating in an insulated finline is a hybrid mode. Since

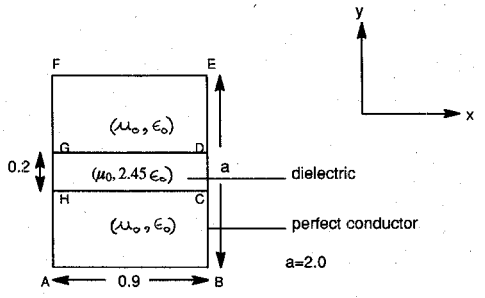

Fig. 10. Centered dielectric slab guide.

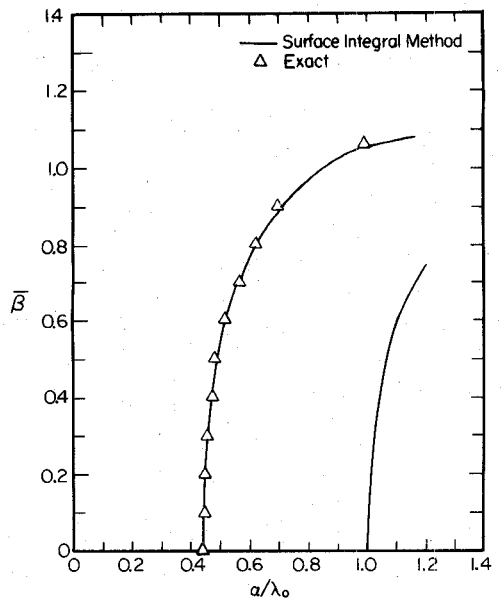

Fig. 11. Propagation constant curve of centered dielectric slab waveguide.

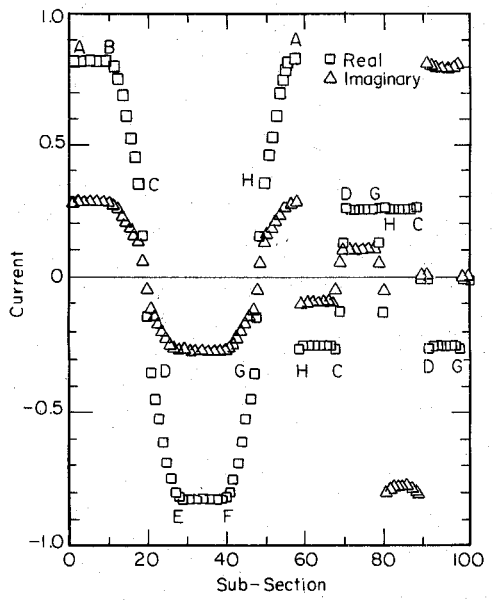

Fig. 12. Eigenvector distribution of centered dielectric slab waveguide.

hybrid modes are characterised by the existence of the axial components of the magnetic and electric fields, they can be represented as a superposition of the TM_z and TE_z modes. However at cutoff ($\beta = 0$), the TM_z and TE_z equations decouple and hence the cutoff frequencies of the insulated finline can be obtained from either the TM_z equations or TE_z equations.

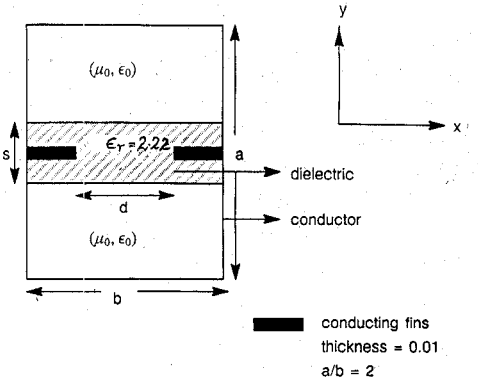

Fig. 13. Insulated finline.

TABLE I
INSULATED FINLINE: DOMINANT MODE NORMALIZED CUT-OFF FREQUENCY ($s/a = 1/16$)

Num.	d/b	b/λ_c	b/λ_c
1	0.125	0.1298	0.1372^{10}
2	0.25	0.1565	0.1630^{10}
3	0.5	0.1945	0.1989^{10}
4	0.75	0.2174	0.2229^{10}

TABLE II
INSULATED FINLINE: DOMINANT MODE NORMALIZED CUT-OFF FREQUENCY ($s/a = 1/8$)

Num.	d/b	b/λ_c	b/λ_c
1	0.125	0.125	0.1285^{10}
2	0.25	0.1477	0.1512^{10}
3	0.5	0.1808	0.1853^{10}
4	0.75	0.2045	0.2090^{10}

Tables I and II give the normalized cut-off wavelengths of the dominant mode, for various dimensions of the insulated finline. These results agree very well with the values obtained using the transverse resonance method [10]. The slight discrepancy in the two results is because insulated fins of finite thickness were used in this paper and zero thickness fins were used in [10].

XI. Discussion and Conclusion

A detailed analysis on the use of the surface integral method to treat dielectric loaded waveguides supporting TM_z and TE_z modes has been explained in this paper. The points on the propagation constant curve were obtained by solving an integro-differential equation. The surface integral method did not produce any spurious modes for the region $0 \leq \bar{\beta} \leq k_0$. However, this wasn't true for the region $k_0 \leq \bar{\beta} \leq k_0\sqrt{\epsilon_r}$ since this method did produce spurious modes in some cases. These spurious modes, however, could easily be identified as being spurious by looking at the eigenvector corresponding to the minimum eigenvalue. A mode can be identified as being spurious using the following two criteria.

The magnetic current vanishes on the surface of a perfect conductor. Since the eigenvector corresponding to the minimum eigenvalue represents the currents on the waveguide, the eigenvector should contain zero magnetic currents at all points where a dielectric touches a conductor. The eigenvector corresponding to some spurious modes, however, produced finite magnetic currents at points where a conductor was in contact with a dielectric. This was the reason why the number of unknowns was not reduced by assuming that zero magnetic currents existed at points where a dielectric was in contact with a conductor. Hence a mode whose eigenvector contains non-vanishing magnetic currents at points where a dielectric touches a conductor can be deemed as being a spurious mode.

There were some spurious modes whose eigenvector did have zero magnetic currents at points where a dielectric touched a conductor. As mentioned earlier, the surface integral method did not produce any spurious modes in the region $0 \leq \bar{\beta} \leq k_0$. The eigenvector in this region represents the variation of the tangential electric and magnetic fields on the surface of the waveguide. Since the distribution of the tangential electric and magnetic fields has to remain the same irrespective of the region, for any mode, the eigenvector distribution in the region $k_0 \leq \bar{\beta} \leq k_0\sqrt{\epsilon_r}$ has to be the same as the eigenvector in the region $0 \leq \bar{\beta} \leq k_0$. This criterion was used to eradicate the rest of the spurious modes (if any).

The surface integral method is a very powerful and useful technique for treating waveguides with complex geometries.

References

[1] M. Swaminathan *et al.*, "Computation of cutoff wavenumbers of TE and TM modes in waveguides of arbitrary cross sections using a surface integral formulation," *IEEE Trans. Microwave Theory Tech.*, vol. 38, no. 2, pp. 154–159, Feb. 1990.

[2] B. E. Spielman and R. F. Harrington, "Waveguides of arbitrary cross section by solution of a nonlinear integral eigenvalue equation," *IEEE Trans. Microwave Theory Tech.*, vol. MTT-20, pp. 578–585, Sept. 1972.

[3] M. Swaminathan, "Analysis of waveguides based on a surface integral formulation," Ph.D. dissertation, Syracuse University, Syracuse, NY, Dec. 1990.

[4] R. F. Harrington, *Time-Harmonic Electromagnetic Fields.* New York: McGraw-Hill, 1961.

[5] ——, *Field Computation by Moment Methods.* New York: Macmillan, 1968.

[6] E. Arvas, S. M. Rao, and T. K. Sarkar, "E-Field solution of TM-scattering from multiple perfectly conducting and lossy dielectric cylinders of arbitrary cross-section," *IEE Proc.*, vol. 133, pt. H, no. 2, pp. 115–121, Apr. 1986.

[7] J. A. Kong, *Theory of Electromagnetic Waves.* New York: Wiley, 1975.

[8] A. R. Djordjevic, T. K. Sarkar, and S. M. Rao, "Analysis of finite conductivity cylindrical conductors excited by axially-independent TM electromagnetic field," *IEEE Trans. Microwave Theory Tech.*, vol. MTT-33, no. 10, pp. 960–966, Oct. 1985.

[9] M. Abramowitz and I. Stegun, *Handbook of Mathematical Functions.* New York: Dover, 1965.

[10] Y.-C. Shih and W. J. R. Hoefer, "Dominant and second-order mode cutoff frequencies in fin lines calculated with a two-dimensional TLM program," *IEEE Trans. Microwave Theory Tech.*, vol. MTT-23, no. 12, pp. 1443–1448, Dec. 1980.

[11] J. A. Kong, *Theory of Electromagnetic Waves.* New York: Wiley, 1975.

[12] M. Abramowitz and I. Stegun, *Handbook of Mathematical Functions.* New York: Dover, 1965.

[13] M. Swaminathan *et al.*, Response to Comments on "Computation of cutoff wavenumbers of TE and TM modes in waveguides of arbitrary cross sections using a surface integral formulation," *Microwave Theory Tech.*, vol. 38, no. 11, Nov. 1990.

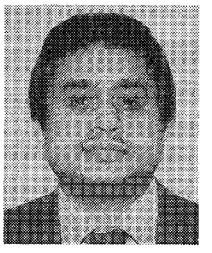

Madhavan Swaminathan (M'91) was born on August 9, 1962 in Madras, India. He received the B.E. degree in electronics and communication from Regional Engineering College, Tiruchi, India, in 1985, and the M.S. and Ph.D. degrees in electrical engineering from Syracuse University in 1989 and 1991, respectively.

He was a Graduate Assistant in the Department of Electrical and Computer Engineering at Syracuse University from 1986–1990. During this period he was made a Fellow of the Northeast Parallel Architectures Center for a period of one year. As a Fellow, he developed algorithms for the solution of large electromagnetic field problems on parallel computers. In 1990 he joined the International Business Machines Corporation, East Fishkill, NY, where he is presently working on the analysis of transmission lines for high speed integrated circuits. His research interests are in the areas of microwave transmission lines, cavity resonators and electromagnetic radiation.

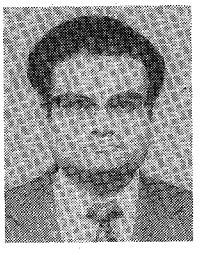

Tapan K. Sarkar (S'69–M'76–SM'81–F'91), was born in Calcutta, India, on August 2, 1948. He received the B.Tech. degree from the Indian Institute of Technology, Kharagpur, India, in 1969, the M.Sc.E. degree from the University of New Brunswick, Fredericton, Canada, in 1971, and the M.S. and Ph.D. degrees from Syracuse University, Syracuse, NY, in 1975.

From 1975 to 1976 he was with the TACO Division of the General Instruments Corporation. He was with the Rochester Institute of Technology, Rochester, NY, from 1976 to 1985. He was a Research Fellow at the Gordon McKay Laboratory, Harvard University, Cambridge, MA, from 1977 to 1978. He is now a Professor in the Department of Electrical and Computer Engineering, Syracuse University, Syracuse, NY. His current research interests deal with numerical solutions of operator equations arising in electromagnetics and signal processing with application to system design. He obtained one of the "best solution" awards in May 1977 at the Rome Air Development Center (RADC) Spectral Estimation Workshop. He has authored or coauthored more than 154 journal articles and conference papers and has written chapters in eight books.

Dr. Sarkar is a registered professional engineer in the state of New York.

He received the Best Paper Award of the IEEE TRANSACTIONS ON ELECTROMAGNETIC COMPATIBILITY in 1979. He was an Associate Editor for feature articles of the *IEEE Antennas and Propagation Society Newsletter*, and he was the Technical Program Chairman for the 1988 IEEE Antennas and Propagation Society International Symposium and URSI Radio Science Meeting. He is an Associate Editor of the IEEE TRANSACTIONS ON ELECTROMAGNETIC COMPATIBILITY and of the *Journal of Electromagnetic Waves and Applications*. He has been appointed U.S. Research Council Representative to many URSI General Assemblies. He is also the Chairman of the Intercommission Working Group of International URSI on Time Domain Metrology. Dr. Sarkar is a member of Sigma Xi and International Union of Radio Science Commissions A and B.

Arlon T. Adams, (M'58–SM'72) received the Ph.D. degree in electrical engineering in 1964 from the University of Michigan, Ann Arbor.

In 1963, he joined the faculty of Syracuse University, Syracuse, NY, where he is currently Professor of Electrical Engineering. During the academic year 1976–1977, he was a Visiting Scholar at the University of California at Berkeley. His current interests are in numerical methods for electromagnetic problems. He is the author of a textbook on electromagnetic theory and coauthor of a textbook on electromagnetic compatibility.